4 Photoinduced nucleation of low temperature hydroperoxy radical chemistry

4.1 Introduction

New particle formation events are well known in the atmosphere, occurring on ~ 90% of days in the coastal U.K. as one example.[1] However the contribution these nucleation events make to the total atmospheric aerosol, and all of the associated climate and air pollution effects, still remains unclear.[2,3] New particle formation has been found to occur nearly everywhere in the atmosphere, and a variety of mechanisms including binary, ternary, and ion-induced heteromolecular homogenous nucleation have been proposed.[4] The large amount of sulfate in aerosols suggests the importance of ternary sulfuric acid-water-ammonia heteromolecular homogenous nucleation,[5,6] but the large organic fractions observed in aerosol are not thought to result from homogenous nucleation except in particular circumstances.[7] In order to better understand the mechanism of homogenous nucleation, both theoretical and experimental investigations have begun on the nanoscale ultrafine clusters which are the precursor to these particles.[8,9]

It is clear that the importance of homogenous nucleation will be regime dependent as models predict orders of magnitude differences in new particle formation rates based on chemical sources and local meterology.[5] The coasts appear to be one area that are highly susceptible to influence from homogeneous nucleation. A recent summary of marine aerosol by O’Dowd and de Leeuw focuses on two possible mechanisms for nucleation: Ternary nucleation of sulfuric acid-water-ammonia mixtures and iodine oxide radical reactions.[10] The first mechanism is one of the well established nucleation mechanisms mentioned previously. The second is interesting because it proposes radical chemistry, i.e., photoinduced chemistry, as part of the nucleation mechanism. A number of observational studies have noted the importance of sunlight for nucleation events to occur, but the focus has been on the radical chemistry converting sulfur species to sulfuric acid,[5] rather than a direct role of the radical in nucleation.

While the details of nucleation models still differ, an important step from the molecular point of view is the formation of a critical cluster. The critical cluster size is reached when a fluctuating collection of molecules begins adding more molecules than it loses and experiences runaway growth leading to a particle. In the atmosphere the existence of radical molecule complexes might help create critical clusters for nucleation. Theoretical work investigated how the complex of the hydroperoxy radical (HO_2) with water (H_2O) might affect aerosol and water droplets, but experimental studies are lacking.[11,12] Work in this lab has looked at an analogous hydrogen bonding complex between HO_2 and methanol (CH_3OH), motivated by the fact that CH_3OH is a common precursor for HO_2 in flash photolysis systems.[13,14]

$$\mathrm{Cl_2} \xrightarrow{hv\ 308\ nm} \mathrm{2Cl} \tag{4.1}$$

$$\mathrm{Cl + CH_3OH \longrightarrow CH_2OH + HCl} \tag{4.2}$$

$$\mathrm{CH_2OH + O_2 \longrightarrow HO_2 + HCHO} \tag{4.3}$$

$$\mathrm{HO_2 + HO_2 \xrightarrow{M} H_2O_2 + O_2} \tag{4.4}$$

$$\mathrm{HO_2 + CH_3OH \rightleftharpoons HO_2{\bullet}CH_3OH} \tag{4.5}$$

$$\mathrm{HO_2 + HO_2{\bullet}CH_3OH \longrightarrow H_2O_2 + O_2 + CH_3OH} \tag{4.6}$$

$$\mathrm{HO_2{\bullet}CH_3OH + CH_3OH \rightleftharpoons HO_2{\bullet}(CH_3OH)_2} \tag{4.7}$$

$$\mathrm{HO_2{\bullet}(CH_3OH)}_n + \mathrm{CH_3OH} \rightleftharpoons \mathrm{HO_2{\bullet}(CH_3OH)}_{n+1} \qquad (4.8)$$

Previous experimental work initially focused on reactions (4.4) – (4.6) and the role of the HO_2• CH_3OH complex on the kinetics of the HO_2 self reaction. The possibility of further complexation as depicted in reactions (4.7) and (4.8) was proposed due to non-linear kinetic dependences as well as the observation of large absorptions attributed to nucleation. This work has further probed the observed nucleation of the HO_2• CH_3OH system, and also explored whether other hydrogen bonding partners of HO_2 might nucleate.

4.2 Experimental

The infrared kinetics spectroscopy (IRKS) apparatus was used during these experiments. Briefly, it consisted of a two meter glass flow cell that was jacketed to allow for temperature control. Chemistry in the cell was initiated by flash photolysis with an excimer laser that made one pass down the length of the cell. Two optical probes, one in the UV and one in the NIR, monitored the time behavior of species in the cell. UV light from a deuterium lamp made one pass through the cell co-aligned and counter-propagating with the photolysis beam. A NIR diode made 30 passes through the cell using spherical Herriott mirrors. A full description of the apparatus has been given previously,[15,16] and it will also be discussed further in Chapter 5.

Two significant changes have been made in the experimental procedures and data analysis. First, wavelength modulation of the NIR probe was not used. Direct absorption provided sufficient sensitivity and a more physically meaningful measurement of the total light extinction. Second, a temperature correction was applied to the data. Chapter 5 discusses the measurements which revealed a discrepancy between the measured temperature and the true temperature. Data originally thought to be at temperatures ranging from 221 – 234 K were actually at 210 – 225 K. This difference is important because [CH_3OH] used was constrained by the vapor pressure of CH_3OH at that particular temperature. In order to compare the [CH_3OH] being used at different temperatures we defined the relative humidity of CH_3OH in equation (4.9) ,

$$RH_{CH3OH} = \frac{[\mathrm{CH_3OH}]}{[\mathrm{CH_3OH}]^*} * 100\% \tag{4.9}$$

where [CH_3OH]* was the vapor pressure of CH_3OH at a particular temperature expressed as a concentration in molecules cm^{-3}. For one or two data sets the temperature offset meant that $RH_{CH3OH} > 100\%$ was used. No difference in the nucleation behavior was observed under these circumstances, but it was suspected that some condensation of CH_3OH on the walls of the flow cell was occurring due to the continued evidence of chemistry and nucleation after the CH_3OH flow had been shut off.

Reagent and bulk flows were all monitored with mass flow controllers. The vapor from liquid reagents was introduced into the flow cell by bubbling nitrogen gas through the reagent as it was held at a fixed temperature. Methanol (V.P. 30 Torr @ 273K), water (V.P. 5.3 Torr at 275 K), and acetone (V.P. 41 Torr @ 263K) were all delivered in this way. Cl_2 (g) was the radical precursor and was also used as a proxy for initial radical concentration ([HO_2]$_0$). Without nucleation present, and at low [CH_3OH] where formation of HO_2• CH_3OH was negligible, [HO_2]$_0$ could be determined by fitting the self reaction of HO_2. It was a general rule that [HO_2]$_0$ • 0.01*[Cl_2]. This relationship was used when nucleation of high [CH_3OH] made it difficult to directly determine [HO_2]$_0$.

A number of different experiments were conducted to explore the nucleation behavior. The dependence of the nucleation on temperature, [CH_3OH], [HO_2]$_0$, and O_2

was examined. Ethane was also added as a precursor to observe the effect another peroxy radical, i.e., $C_2H_5O_2$, had on the nucleation. H_2O and acetone were also added to see how other hydrogen bonding partners of HO_2 affected the results.

4.3 Results

There was a large extinction of the light from both the UV and NIR probes under the right conditions of temperature, [CH_3OH], and [HO_2]$_0$. The different behavior observed by the two probes provided clues about the size of the particles. Some of the chemical species present, i.e., H_2O_2 and HCl, could be ruled out as important to nucleation by substituting $C_2H_5O_2$ chemistry. Without O_2 much greater nucleation was observed, suggesting a completely different mechanism occurs under those conditions. Nucleation was also observed in the presence of acetone but not with H_2O.

4.3.1 UV absorption

The UV absorption signal for the HO_2 self reaction, at 222 K and $[HO_2]_0 = 1.0 \times 10^{14}$ molecules cm^{-3}, is shown in **Figure 4-1** as a function of [CH_3OH]. The inset shows the standard time window for observing the reaction, and the time trace as the [CH_3OH] was raised to 6.9×10^{15} molecules cm^{-3}. Rather than the signal continuing to return to baseline as the reaction proceeded, a new large absorbance started growing in.

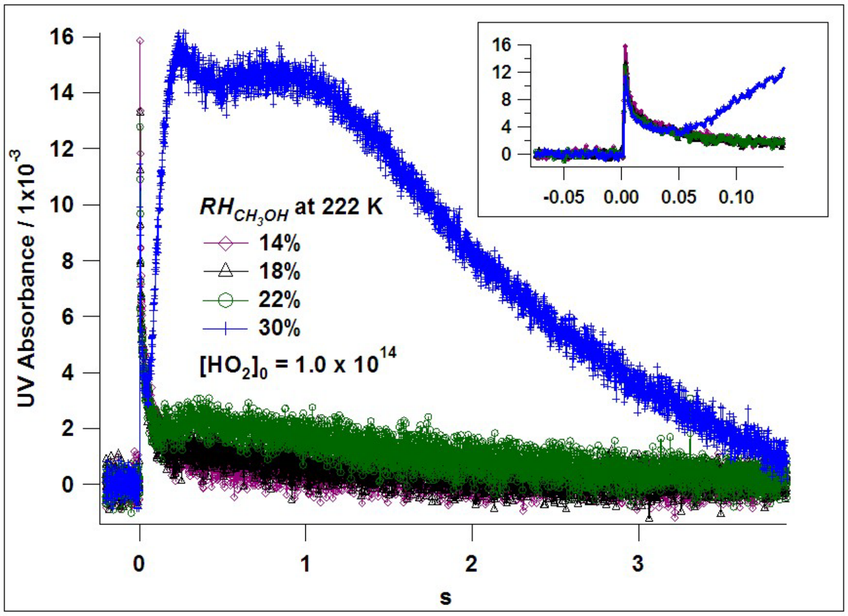

Figure 4-1. UV absorbance from the HO_2 self reaction and the unexpected large absorbance at longer time scales. Inset shows how the same data appeared on the time scale over which the HO_2 self reaction was normally observed.

The rest of the figure shows what the data looked like on a longer time scale; the absorbance continues to grow and remains high for seconds until the pump out of the flow cell starts to remove the absorber. This behavior was also observed at the lower [CH_3OH] of 5.1 x 10^{15} molecule cm^{-3}, only later in time and with less intensity, making it undetectable in the standard time window of the HO_2 self reaction.

4.3.2 Temperature dependence

The large absorption observed in the UV appears to be total extinction due to a phase change, i.e., aerosol formation, than to pure absorption alone. A further study explored whether a temperature change resulted in a sharp or gradual onset of the extinction. A sharp onset would be consistent with a phase change process, while a more gradual dependence might implicate other chemistry. **Figure 4-2** shows the observed extinction in both the UV and the NIR as the temperature of the cell was lowered and then raised from 225 – 216 K and back again at [CH_3OH] = 6.6 x 10^{15} (RH_{CH3OH} varies over 22 – 60% from 225 – 216 K) and $[HO_2]_0 = 1.2 \times 10^{14}$ molecules cm^{-3}. The red 225 K trace showed no sign of nucleation by either probe. In the NIR there was a strange baseline shape at times < 1 s, but it was not related to the aerosol. At 224 K there was an indication of the aerosol in the NIR, but not in the UV. Since the NIR had a much longer pathlength it was more sensitive to the presence of the aerosol. By 223 and 222 K the extinction was very obvious in both probes although the trends were different in the NIR and the UV. Then at 216 K large oscillations appeared that may have been caused by optical resonance between the wavelength and particle size, or by dynamical flow effects. Finally, when the cell was allowed to warm back to 225 K the baselines returned to their original levels, as seen in the blue trace of **Figure 4-2**. There was no evidence of hysteresis or of previously formed particles seeding new particles. This clear temperature dependence and the absence of hysteresis confirmed that aerosol formation was the cause of the light extinction at both wavelengths.

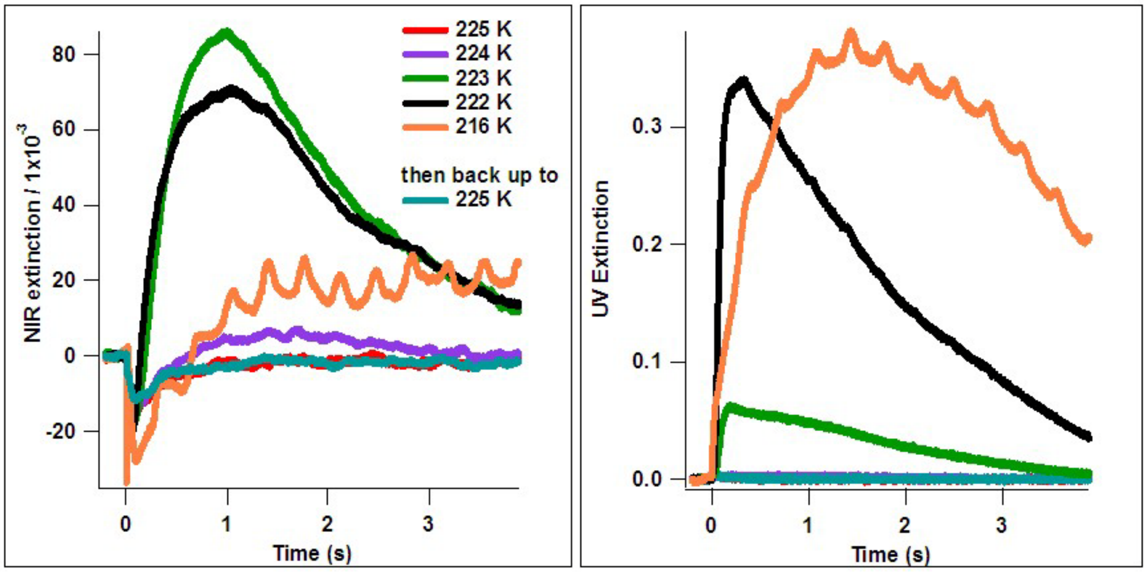

Figure 4-2. Temperature dependence of the extinction in both the NIR and UV. Lowering the temperature one or two degrees led to an immediate appearance of the extinction supporting an aerosol formation hypothesis. No hysteresis was observed in the system as the temperature returned to 225 K.

4.3.3 CH_3OH dependence

Not many species were available to form the bulk of the aerosol; N_2, O_2, Cl_2, and CH_3OH were the only precursors in the system, and only CH_3OH had the ability to condense under the conditions in the cell. **Figure 4-3** shows the UV extinction signal as the [CH_3OH] was increased at a constant temperature of 222 K. A clear dependence on the [CH_3OH] was observed. Additional CH_3OH did not affect the precursor chemistry shown in reactions (4.1) – (4.3) because the reaction of Cl with CH_3OH was already occurring under a large excess of CH_3OH. In order for the additional CH_3OH to influence the observed extinction it had to be contributing to the growth or formation of the aerosol. The strong dependence of the extinction on [CH_3OH] not only indicated that concentration plays a role in determining the number and size of particles, but also that CH_3OH was the major component of the newly formed aerosol.

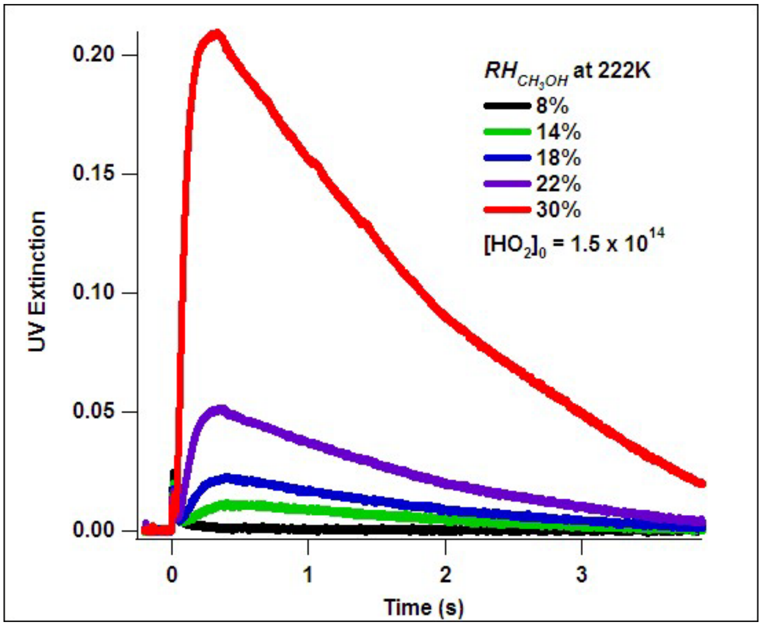

Figure 4-3. Dependence of the UV extinction on CH_3OH concentration. A large increase in extinction was observed for small changes in CH_3OH.

A quantitative interpretation of this data is difficult because both the size and number of particles were changing in time due to growth, agglomeration, and removal from the flow cell by the vacuum pump. Despite this, the large change in extinction observed with only a small increase in [CH_3OH] might provide insight as to the underlying mechanism of the nucleation. **Figure 4-4** shows the dependence of the peak UV extinction on [CH_3OH] at three different initial radical concentrations. Both a power law and 2nd-order polynomial expression fit the data well (the polynomial fit is shown), but no quantitatively consistent dependence was observed under the different radical conditions.

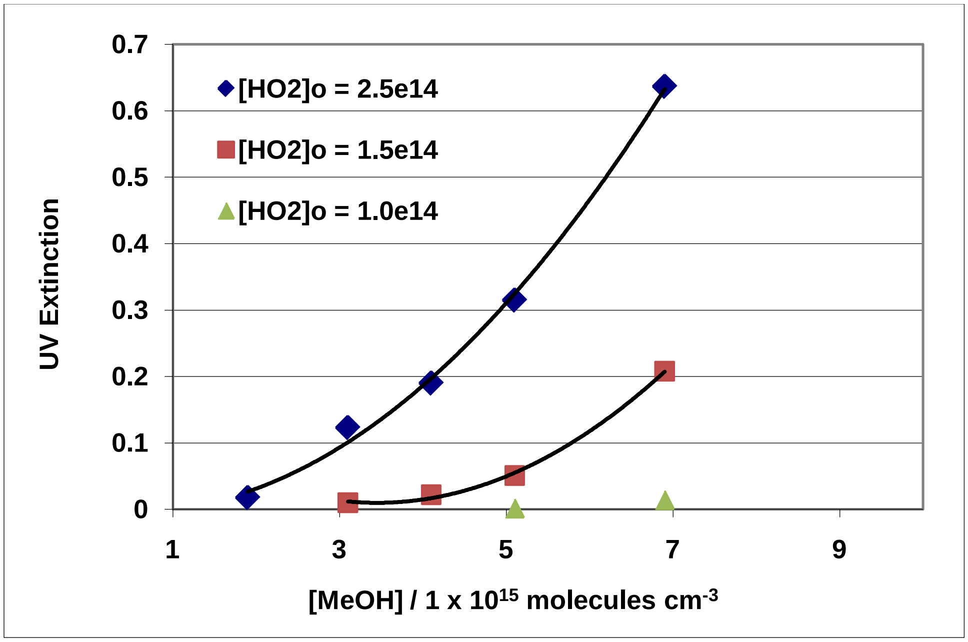

Figure 4-4. Dependence of the peak UV extinction on [CH_3OH] at three different initial radical concentrations

Without further assumptions about either the size distribution or number of particles, no conclusions about the nucleation mechanism were drawn from the quantitative dependence of the extinction on [CH_3OH].

4.3.4 Radical dependence

Nucleation only occurred after the photolysis pulse indicating radical chemistry was a necessary part of initiating particle formation. When starting at low radical concentrations ($[HO_2]_0 < 5 \times 10^{13}$ molecules cm^{-3}), the extinction in both the UV and NIR increased as a function of initial radical concentration, as shown in **Figure 4-5**. The data shown were taken at 224 K and $[CH_3OH] = 3.15 \times 10^{16}$ molecules cm^{-3} (> 100% RH_{CH3OH}), but as mentioned in the experimental section, the nucleation behavior was no different in this case because of the RH_{CH3OH} > 100%. No strange baseline or non-photoinduced nucleation behavior was seen.

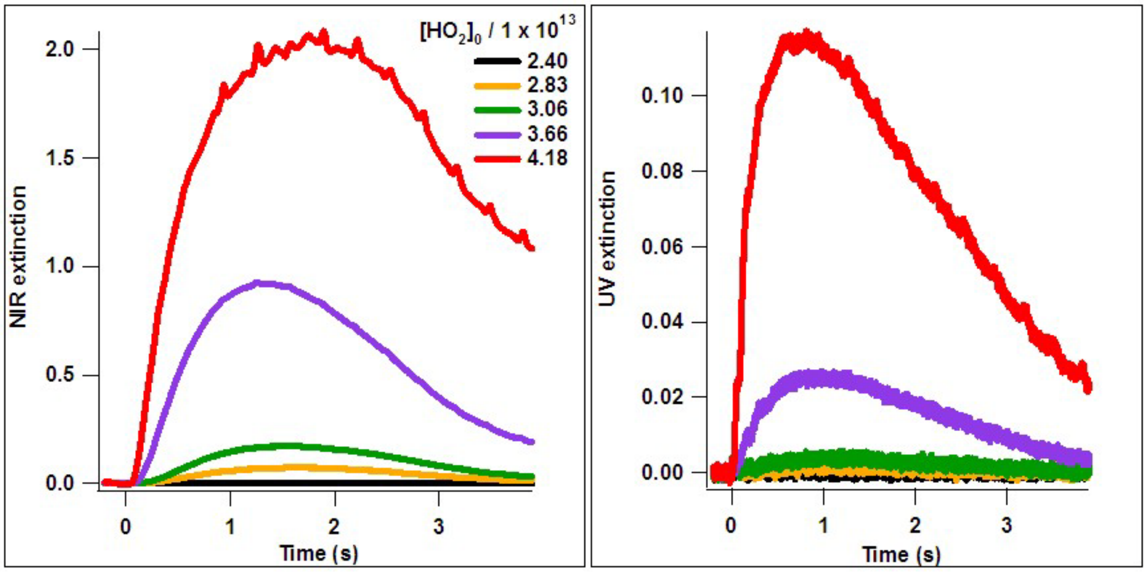

Figure 4-5. Extinction in both the NIR and UV increases as a function of initial radical concentration when radical concentration was < 5 x 10^{13} molecules cm^{-3}.

The peak extinction was very sensitive to $[HO_2]_0$, and **Figure 4-5** shows the large changes in extinction for small changes in $[HO_2]_0$. Unfortunately, as with the $[CH_3OH]$ dependence, no reliable quantitative dependence on $[HO_2]_0$ was determined. **Figure 4-6** plots the peak UV extinction vs. $[HO_2]_0$ for various RH_{CH3OH}. Some of the data appears to have a linear dependence on $[HO_2]_0$, but the trends were not taken over a large enough range to be certain.

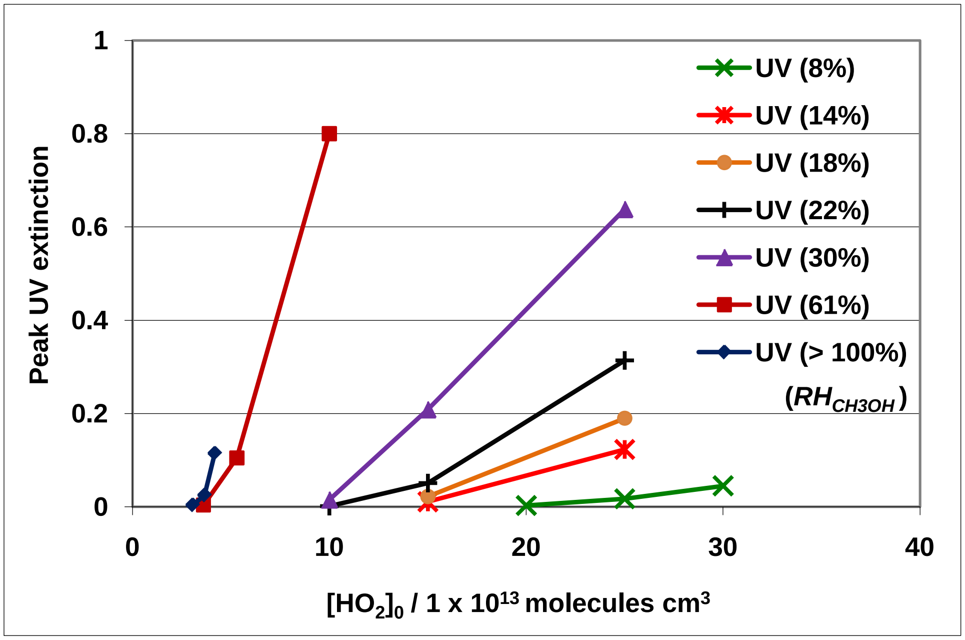

Figure 4-6. Peak UV extinction as a function of initial radical concentration for various RH_{CH3OH}. Lines are only to guide the eye.

The qualitative behavior followed the expected trend; at the lowest RH_{CH3OH} (given in parenthesis in the chart legend) the largest $[HO_2]_0$ was needed to see any nucleation, and as RH_{CH3OH} increased progressively less $[HO_2]_0$ was needed to observe the same amount of extinction. Combining the qualitative observation of increased extinction at increased initial radical with the fact that photolysis was necessary for nucleation, confirmed that radical chemistry was the seed for particle formation.

4.3.5 UV vs NIR dependences

In contrast to data taken at lower $[HO_2]_0$ where the UV and NIR extinctions have a similar dependence on initial radical concentration (**Figure 4-5**), the behavior observed by the two probes started to diverge when $[HO_2]_0$ was raised. **Figure 4-7** compares the UV and NIR extinction as $[HO_2]_0$ was raised above 5 x 10^{13} molecules cm^{-3} at 222 K and

RH_{CH3OH} = 61%. At first both the UV and NIR extinctions increased when $[HO_2]_0$ was raised from 3.6 x $10^{13} \rightarrow$ 5.3 x 10^{13}, and the higher sensitivity of the NIR detected nucleation even when the UV did not. But at the highest $[HO_2]_0$ the NIR extinction decreased while the UV increased dramatically and started rippling behavior. The timing of the peak extinction in the UV was also relatively constant while the NIR peak appeared earlier and earlier as $[HO_2]_0$ went up.

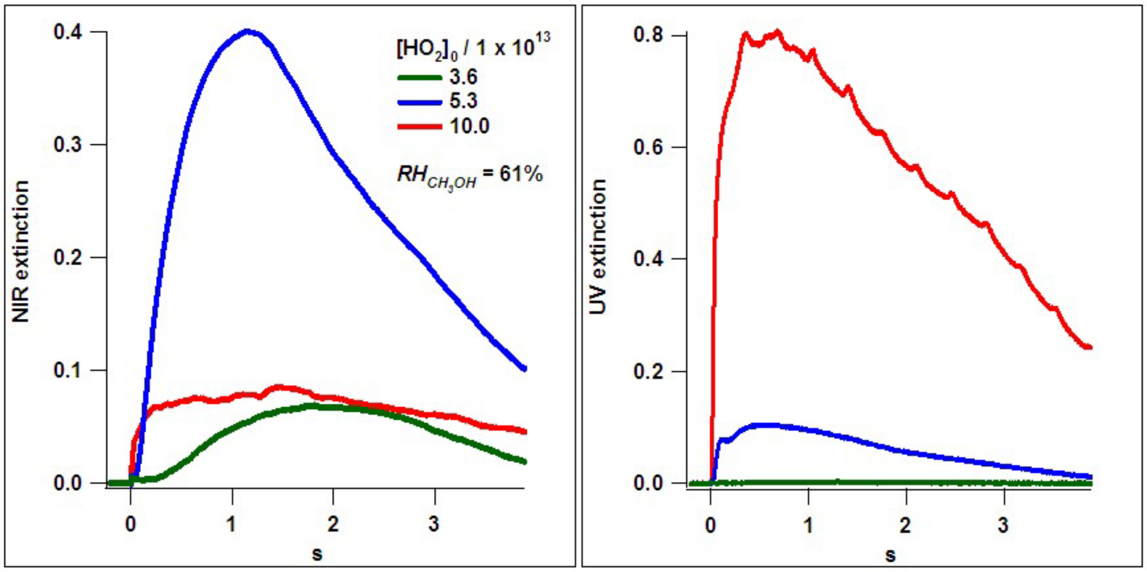

Figure 4-7. Comparison of extinction between the UV and NIR at higher $[HO_2]_0$. NIR extinction was reduced past a certain amount of $[HO_2]_0$.

Increasing the amount of $[HO_2]_0$ seed increases the total number of aerosol possible, but the individual size of each aerosol may decrease. A shift in the size distribution of the aerosol could explain the difference in the extinction observed by the two probes as smaller particles would not extinguish the longer wavelength NIR probe as efficiently as the shorter wavelength UV. Large particles would also take longer to grow, hence the time dependence seen in the NIR as well.

4.3.6 $C_2H_5O_2$

Changing the chemistry of the mixture was a way to probe what was responsible for seeding the particles. **Figure 4-8** shows the effect of adding in ethane (C_2H_6) to create $C_2H_5O_2$ through reactions (4.10) and (4.11).

$$\mathrm{Cl} + \mathrm{C_2H_6} \longrightarrow \mathrm{C_2H_5} + \mathrm{HCl} \tag{4.10}$$

$$\mathrm{C_2H_5} + \mathrm{O_2} \xrightarrow{M} \mathrm{C_2H_5O_2} \tag{4.11}$$

Competition between ethane and CH_3OH for the radical chlorine (Cl) atoms dictates the amount of $C_2H_5O_2$ vs. HO_2 produced. The rate constant for each reaction is very similar ($\sim 5 \times 10^{-11}$ cm^3 molecule^{-1} s^{-1})[17] so the amount of each product formed is in proportion to the amount of each precursor. A control containing no CH_3OH, 8.0×10^{16} molecules cm^{-3} ethane, and an initial radical concentration of 1.0×10^{14} molecules cm^{-3} was measured as well. Without CH_3OH no nucleation should have been possible because it made up the bulk of the particle. The yellow trace represents this control run in **Figure 4-8,** and lies behind those containing methanol showing no sign of nucleation in either the NIR or UV. Next CH_3OH was added in and ethane was reduced until it was nine times the concentration of CH_3OH. This data is the purple trace and looks exactly like the control run without CH_3OH; i.e., no nucleation was observed by either probe for this run either. At an ethane concentration of 2.5×10^{16} molecules cm^{-3} ($\sim 3 \times [CH_3OH]$) the UV still showed no nucleation, but the more sensitive NIR showed a peak at later times. As ethane was reduced again, the NIR reached its largest extinction while the UV was just beginning to be visible. The UV extinction continued to get larger with the further reduction of ethane while the NIR had already peaked and was getting smaller although the rise time of the signal continued to get faster.

These data also provided another good example of the NIR dependence at large $[HO_2]_0$. As the amount of CH_3OH chemistry increased (by reducing the competition from ethane), the amount of radical seed also increased, which led to an initial rise followed by a decline in the NIR peak extinction.

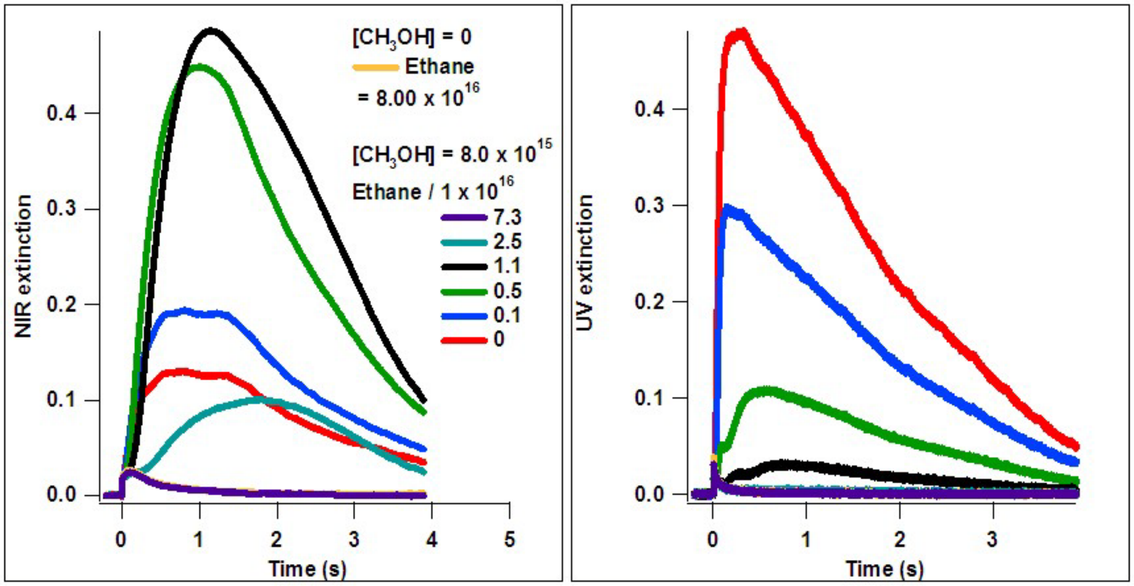

Figure 4-8. Changing the chemistry of the nucleation to include $C_2H_5O_2$ provided some insight into the seed molecule. The different behavior of the UV and NIR at larger radical concentrations was also clearly observed here as well.

The precursor chemistry common to both CH_3OH and ethane are reactions (4.2) and (4.10) where H atom abstraction by Cl forms HCl. Regardless of the precursor ratio of ethane and CH_3OH the same amount of HCl will be produced at a given initial radical concentration. In the data where CH_3OH was present (making nucleation possible), comparing the data at the highest ethane (purple trace) of **Figure 4-8** to all of the subsequent traces showed that HCl was not the nucleation seed. No nucleation was observed in the purple, but it was later on when the only change was the precursor ratio, but as just discussed the precursor ratio does not change the HCl concentration. A further analysis of concentrations from the light blue trace ($[C_2H_6 = 2.5 \times 10^{16}$ molecules $cm^{-3})$

suggests that another species in the HO_2• CH_3OH chemistry can also be ruled out as the nucleation seed: HOOH. For this sample, ~ 1/4 of the 1 x 10^{14} radicals will be HO_2 based on the precursor ratio of ethane and CH_3OH. This $[HO_2]_0 = 2.5 \times 10^{13}$ was close to the lower limit at which nucleation was observed in any of the previous data, as can be seen in **Figure 4-5**. In this case however ~ 90% of the HO_2 will not self react to form HOOH, but will react instead with $C_2H_5O_2$, lowering the concentration of HOOH by ~ 1 order of magnitude. This suggests that HOOH was also not the radical seed; otherwise data at lower radical concentrations where ethane was not present and all of the HO_2 forms HOOH would have shown nucleation.

4.3.7 Acetone and Water

Nucleation was investigated in the presence of other HO_2 hydrogen bonding partners as well. It is well known that HO_2 forms a hydrogen bonded complex with water,[18-20] and if the HO_2• CH_3OH complex is the seed of the observed nucleation, it is possible that a HO_2• H_2O complex might also prompt nucleation. At both 273 and 254 K, with up to 1.5 x 10^{16} molecules cm^{-3} of H_2O, no nucleation was observed. Theoretical work from a few groups has also suggested that acetone might form a complex with HO_2 at low temperature.[21-23] During work with Professor Fred Grieman, nucleation was observed at high acetone concentrations while measuring the K_{eq} for the reaction of HO_2 with acetone at temperatures of 222 and 213 K.[24] In these experiments nucleation was not observed for samples that only included CH_3OH, the addition of acetone was necessary to observe the nucleation.

4.3.8 Nucleation with no O_2 present

Nucleation from mixtures of Cl_2/CH_3OH, but without O_2, exhibited even greater extinction than those with O_2. The observed nucleation was so much greater that it was likely due to a very different process than the one observed with O_2. In this case it was likely that polymerization reactions of the CH_2OH radical were dominant. Similar behavior with and without O_2 has been observed in photoinduced nucleation of aldehyde systems.[25,26]

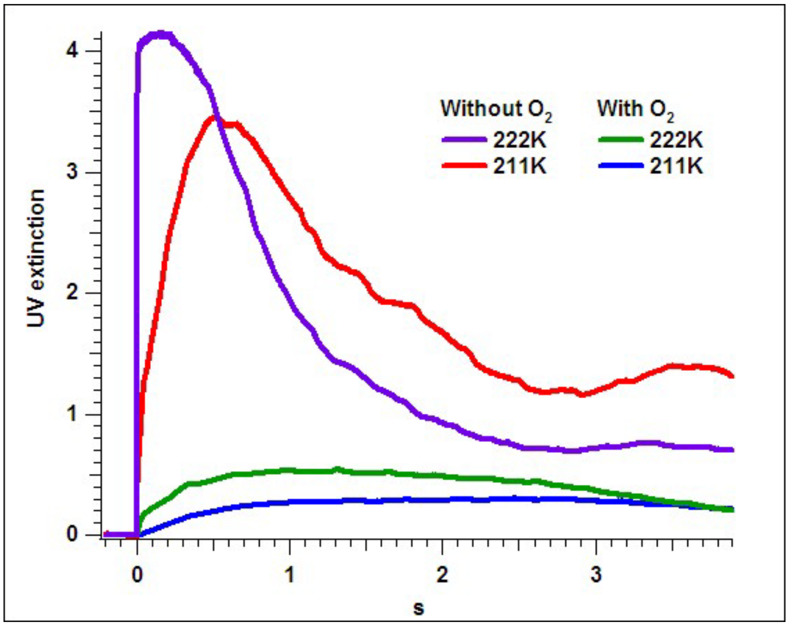

Figure 4-9. Greater extinction was observed in the absence of O_2, suggesting polymerization of the CH_2OH radical.

When O_2 is present at concentrations of ~ 1 x 10^{18} molecules cm^{-3} the reaction of CH_2OH with O_2 happens very quickly (10^7 s^{-1}). Reaction between CH_2OH and CH_3OH would have had to occur at the gas kinetic rate to have any chance of being competitive with the O_2 reaction pathways (10^6 s^{-1}). Therefore it is likely that the observed nucleation had different seeds in the absence and presence of O_2. Rate constants are also not nearly as sensitive to temperature as phase changes. Since even one degree Kelvin can mean a difference between no observed nucleation and large extinctions, it is unlikely the $CH_2OH + CH_3OH$ reaction is suddenly favored over the $CH_2OH + O_2$ reaction.

4.4 Discussion

4.4.1 The nucleation dependence on temperature, [CH_3OH], and [HO_2]$_0$

The large extinctions observed in both the UV and NIR are thought to be caused by aerosol formation due to their strong non-linear dependence on temperature, [CH_3OH], and [HO_2]$_0$. The [CH_3OH] dependence data are convincing evidence that CH_3OH made up the bulk of the particles, and the [HO_2]$_0$ dependence is confirmation that radical chemistry provided the nucleation seed. Increasing the [CH_3OH] provided more material for the aerosol to form and resulted in greater extinction. Likewise increasing [HO_2]$_0$ provided more seeds for nucleating aerosol and led to greater extinction as long as an excess of CH_3OH existed.

Some of the most intriguing potential from these experiments comes from the observed difference in extinction between the UV and the NIR as the nucleation seed increased. The decrease in the NIR extinction as [HO_2]$_0$ increased (shown in **Figure 4-7** and **4-8**) can be explained by a shift in the particle size distribution. More seed leads to the growth of a greater number of smaller particles, but fewer larger ones. The resulting extinctions in the NIR and UV were an example of how different wavelengths of light can be used to probe different size scales of nucleation and particle growth simultaneously. The time delay in the NIR peak at the lowest concentrations of [CH_3OH] and [HO_2]$_0$, in comparison to the uniform time dependence of the UV, is another example of how the different wavelengths can focus on different stages of growth. The different behaviors also suggest that specific aspects of nucleation can be targeted by using different chemistry regimes, i.e., different [CH_3OH] and [HO_2]$_0$.

The strong oscillations observed in the temperature dependence data of **Figure 4-2** were another optical effect that might be exploited to get information about the size distribution of the aerosol. The wiggles in the extinction are expected from Mie theory when particles approach the size of the wavelength of the incident light.[27] The very similar period of the wiggles for both the NIR and UV in **Figure 4-2** might also indicate another explanation, such as a dynamical effect from the flow system. For example, the pump out of aerosols and the pump in of fresh CH_3OH flow lead to an oscillation in the growth and disappearance of the aerosol. However, the fact that the oscillations appear in other data, but not always in both the UV and NIR make a flow explanation less convincing. A true analysis of the data using Mie theory requires some estimation of the particle number and size distribution and proposed experiments are described in the Future Work section.

4.4.2 Chemistry changes and seed possibilities

The work discussed so far reports the growth of already formed aerosol, not the actual nucleation process. Nucleation occurs in clusters too small to observe with the present experiment, so only the already formed aerosols were large enough to cause extinction of the light. A different way to investigate the actual nucleation process was also tried by changing the initiation chemistry leading up to it. The $C_2H_5O_2$ work ruled out HOOH and HCl as the species acting as a nucleation seed, but still left HO_2 and HCHO, as both were made in equal amounts when HO_2 was formed. With these species present there are two possible mechanisms for nucleation. In the first, shown in reaction

(4.8), the HO_2• CH_3OH complex can continue to add CH_3OH until a critical cluster size is passed, leading to particle formation. Another version of this mechanism involves the interaction of multiple complexes to help form the critical cluster, but is otherwise the same. The second mechanism is a binary nucleation process between the HCHO and CH_3OH. In many cases during these experiments RH_{CH3OH} was less than 100% which precludes homomolecular homogenous nucleation from occurring. However the mixture of HCHO and CH_3OH could have a much lower vapor pressure leading to their condensation in heteromolecular homogenous nucleation. It has been observed in the case of H_2O-H_2SO_4 mixtures that even trace amounts of H_2SO_4 can greatly increase nucleation.[28]

The concentrations used in this experiment are not directly applicable to the atmosphere. Even if the HO_2• CH_3OH was proven to be the seed, it might have only limited direct atmospheric importance since no nucleation was observed in the presence of the most important complex of HO_2 in the atmosphere, HO_2• H_2O. Still one interesting part of this work is the incorporation of a very light molecular weight species into aerosol. Atmospheric chemistry models consistently under predict aerosol concentrations in comparison to what is actually measured.[29] One reason for this is that low molecular weight species have been largely ignored based on their Henry's law constants. Work on isoprene oxidation and aerosol formation has shown that low molecular weight glyoxal forms aerosol,[30] and recent work on the photolysis of acetylene shows that it too can form aerosol under the right conditions.[31] Even more species are likely to be important for a variety of reasons, and heterogeneous radical chemistry may provide one way to further incorporate lower molecular weight species into pre-existing particles. The radical-molecule complex of this work may not be relevant to atmospheric nucleation specifically, but it may provide another route for pre-existing particle growth.

4.4.3 Future experiments

Two different experiments could help resolve the nucleation mechanism. The first would be to simply add a small amount of HCHO to the exact same flow and temperature conditions used in this work to see if the trace HCHO leads to binary nucleation. An alternative experiment is to generate HO_2 in such a way that HCHO is not also created. One possibility to generate HO_2 is photolysis of H_2O_2. Another common source of HO_2, $F_2/H_2/O_2$ chemistry, would be complicated by the F atom reacting with the CH_3OH and potentially leading to HCHO again.

Other experiments would also be useful to investigate the number and size distributions of the observed aerosol. For instance, the introduction of a sample from the flow cell exhaust into a particle counter would help to characterize the aerosol. Experimentally it would be difficult to maintain the low temperature throughout the system to prevent evaporation of the aerosol, but information on total particle number would help greatly in interpreting the measured extinctions.

4.5 Conclusion

Low temperature experiments on the HO_2 self reaction led to surprising observations of photoinduced nucleation of aerosols. Varying the precursor chemistry allowed definitive assignment of CH_3OH as the main condensing species, and either HO_2 or HCHO chemistry as the nucleation seed. The different response of the extinction in the UV and NIR probes gave an indication of the size regime of the aerosol being formed. Although the specific system is probably not directly relevant to the atmosphere given the concentrations used, the possibility of radical induced nucleation or binary nucleation of two low molecular weight species could be important analogs to processes currently overlooked in aerosol models.

4.6 References

(1) O'Dowd, C. D.; Hameri, K.; Makela, J. M.; Pirjola, L.; Kulmala, M.; Jennings, S. G.; Berresheim, H.; Hansson, H. C.; de Leeuw, G.; Kunz, G. J.; Allen, A. G.; Hewitt, C. N.; Jackson, A.; Viisanen, Y.; Hoffmann, T. *Journal of Geophysical Research-Atmospheres* **2002**, *107*.

(2) Laakso, L.; Anttila, T.; Lehtinen, K. E. J.; Aalto, P. P.; Kulmala, M.; Horrak, U.; Paatero, J.; Hanke, M.; Arnold, F. *Atmospheric Chemistry and Physics* **2004**, *4*, 2353.

(3) Poschl, U. *Angewandte Chemie-International Edition* **2005**, *44*, 7520.

(4) Kulmala, M. *Science* **2003**, *302*, 1000.

(5) Hegg, D. A.; Baker, M. B. *Reports on Progress in Physics* **2009**, *72*, 21.

(6) Textor, C.; Schulz, M.; Guibert, S.; Kinne, S.; Balkanski, Y.; Bauer, S.; Berntsen, T.; Berglen, T.; Boucher, O.; Chin, M.; Dentener, F.; Diehl, T.; Easter, R.; Feichter, H.; Fillmore, D.; Ghan, S.; Ginoux, P.; Gong, S.; Kristjansson, J. E.; Krol, M.; Lauer, A.; Lamarque, J. F.; Liu, X.; Montanaro, V.; Myhre, G.; Penner, J.; Pitari, G.; Reddy, S.; Seland, O.; Stier, P.; Takemura, T.; Tie, X. *Atmospheric Chemistry and Physics* **2006**, *6*, 1777.

(7) Kanakidou, M.; Seinfeld, J. H.; Pandis, S. N.; Barnes, I.; Dentener, F. J.; Facchini, M. C.; Van Dingenen, R.; Ervens, B.; Nenes, A.; Nielsen, C. J.; Swietlicki, E.; Putaud, J. P.; Balkanski, Y.; Fuzzi, S.; Horth, J.; Moortgat, G. K.; Winterhalter, R.; Myhre, C. E. L.; Tsigaridis, K.; Vignati, E.; Stephanou, E. G.; Wilson, J. *Atmospheric Chemistry and Physics* **2005**, *5*, 1053.

(8) Kathmann, S. M.; Schenter, G. K.; Garrett, B. C.; Chen, B.; Siepmann, J. I. *Journal of Physical Chemistry C* **2009**, *113*, 10354.

(9) Kulmala, M.; Kerminen, V. M. *Atmospheric Research* **2008**, *90*, 132.

(10) O'Dowd, C. D.; De Leeuw, G. “Marine aerosol production: a review of the current knowledge”, 2007.

(11) Belair, S. D.; Hernandez, H.; Francisco, J. S. *Journal of the American Chemical Society* **2004**, *126*, 3024.

(12) Shi, Q. C.; Belair, S. D.; Francisco, J. S.; Kais, S. *Proceedings of the National Academy of Sciences of the United States of America* **2003**, *100*, 9686.

(13) Christensen, L. E.; Okumura, M.; Hansen, J. C.; Sander, S. P.; Francisco, J. S. *Journal of Physical Chemistry A* **2006**, *110*, 6948.

(14) Christensen, L. E.; Okumura, M.; Sander, S. P.; Salawitch, R. J.; Toon, G. C.; Sen, B.; Blavier, J. F.; Jucks, K. W. *Geophysical Research Letters* **2002**, *29*.

(15) Christensen, L. Laboratory studies of atmospherically important gas-phase peroxy radical reactions. , California Insitute of Technology, 2003.

(16) Christensen, L. E.; Okumura, M.; Sander, S. P.; Friedl, R. R.; Miller, C. E.; Sloan, J. J. *Journal of Physical Chemistry A* **2004**, *108*, 80.

(17) Sander, S. P.; Finlayson-Pitts, B. J.; Friedl, R. R.; Golden, D. M.; Huie, R. E.; Kolb, C. E.; Kurylo, M. J.; Molina, M. J.; Moortgat, G. K.; Orkin, V. L.; Ravishankara, A. R. “JPL 2006: Chemical Kinetics and Photochemical Data for Use in Atmospheric Studies, Evaluation No. 15, JPL Publication 06-2, Jet Propulsion Lab,” 2006.

(18) Hamilton, E. J. *Journal of Chemical Physics* **1975**, *63*, 3682.

(19) Hamilton, E. J.; Lii, R. R. *International Journal of Chemical Kinetics* **1977**, *9*, 875.

(20) Suma, K.; Sumiyoshi, Y.; Endo, Y. *Science* **2006**, *311*, 1278.

(21) Cours, T.; Canneaux, S.; Bohr, F. *International Journal of Quantum Chemistry* **2007**, *107*, 1344.

(22) Hermans, I.; Muller, J. F.; Nguyen, T. L.; Jacobs, P. A.; Peeters, J. *Journal of Physical Chemistry A* **2005**, *109*, 4303.

(23) Hermans, I.; Nguyen, T. L.; Jacobs, P. A.; Peeters, J. *Journal of the American Chemical Society* **2004**, *126*, 9908.

(24) Grieman, F. J., Noell, A.C., Okumura, M., Sander, S.P. **Manuscript in preparation**.

(25) Dubtsov, S. N.; Dultseva, G. G.; Dultsev, E. N.; Skubnevskaya, G. I. *Journal of Physical Chemistry B* **2006**, *110*, 645.

(26) Skubnevskaya, G. I.; Dubtsov, S. N.; Dultsev, E. N.; Dultseva, G. G.; Tsang, W. *Journal of Physical Chemistry B* **2004**, *108*, 11393.

(27) Seinfeld, J. H., Pandis, S.N. Atmospheric Chemistry and Physics; John Wiley and Sons: New York, 1998; pp 82.

(28) Ball, S. M.; Hanson, D. R.; Eisele, F. L.; McMurry, P. H. *Journal of Geophysical Research-Atmospheres* **1999**, *104*, 23709.

(29) Volkamer, R.; Jimenez, J. L.; San Martini, F.; Dzepina, K.; Zhang, Q.; Salcedo, D.; Molina, L. T.; Worsnop, D. R.; Molina, M. J. *Geophysical Research Letters* **2006**, *33*.

(30) Kroll, J. H.; Ng, N. L.; Murphy, S. M.; Flagan, R. C.; Seinfeld, J. H. *Environmental Science & Technology* **2006**, *40*, 1869.

(31) Volkamer, R.; Ziemann, P. J.; Molina, M. J. *Atmospheric Chemistry and Physics* **2009**, *9*, 1907.